Temporal covariation of epibacterial community and surface metabolome in the Mediterranean seaweed holobiont Taonia atomaria

Benoît Paix, Ahlem Othmani, Didier Debroas, Gérald Culioli, Jean-François Briand

environmental microbiology

Environmental Microbiology (2019) **21**(9), 3346–3363 doi:10.1111/1462-2920.14617

Temporal covariation of epibacterial community and surface metabolome in the Mediterranean seaweed holobiont *Taonia atomaria*

Benoît Paix,[1†] **Ahlem Othmani**,[1†] **Didier Debroas**,[2] **Gérald Culioli**[1*] **and Jean-François Briand**[1*]

[1]*Université de Toulon, Laboratoire MAPIEM, EA 4323, Toulon, France.*

[2]*Université Clermont Auvergne, CNRS, Laboratoire Microorganismes: Génome et Environnement, UMR 6023, Clermont–Ferrand, France.*

Summary

An integrative multi-omics approach allowed monthly variations for a year of the surface metabolome and the epibacterial community of the Mediterranean Phaeophyceae *Taonia atomaria* to be investigated. The LC–MS-based metabolomics and 16S rDNA metabarcoding data sets were integrated in a multivariate meta-omics analysis (multi-block PLS-DA from the MixOmic DIABLO analysis) showing a strong seasonal covariation (Mantel test: $p < 0.01$). A network based on positive and negative correlations between the two data sets revealed two clusters of variables, one relative to the 'spring period' and a second to the 'summer period'. The 'spring period' cluster was mainly characterized by dipeptides positively correlated with a single bacterial taxon of the Alteromonadaceae family (BD1-7 clade). Moreover, 'summer' dominant epibacterial taxa from the second cluster (including Erythrobacteraceae, Rhodospirillaceae, Oceanospirillaceae and Flammeovirgaceae) showed positive correlations with few metabolites known as macroalgal antifouling defences [e.g. dimethylsulphoniopropionate (DMSP) and proline] which exhibited a key role within the correlation network. Despite a core community that represents a significant part of the total epibacteria, changes in the microbiota structure associated with surface metabolome variations suggested that both environment and algal host shape the bacterial surface microbiota.

Received 15 January, 2019; accepted 31 March, 2019. *For correspondence. E-mail briand@univ-tln.fr. E-mail culioli@univ-tln.fr; Tel. 33 (0)4 94 14 67 60. †These authors contributed equally to this work.

Introduction

The major ecological importance of marine macroalgae in coastal ecosystems no longer needs to be demonstrated, as these organisms play several crucial roles (e.g. oxygen production, source of food and energy, and building and protective habitats). As for all immersed surfaces in seawater, seaweeds are colonized by microbial communities. Recently, several studies on the diversity and functions of algal surface-associated microbial communities led to a modification in the conceptual consideration of the relationships between these microbiomes and their basibionts. Diversified and species-specific bacterial communities have been described on seaweeds found in tropical coral reefs and the authors have proposed to apply the concept of holobionts to such biological systems. Primarily developed for corals (Rosenberg *et al*., 2007, Barott *et al*., 2011), the concept of the holobiont and hologenome has been rapidly extended to many multicellular eukaryotic hosts from plants to animals, including humans (Bordenstein and Theis, 2015). Recent advances in discussions of the concept of holobiont (Theis *et al*., 2016) confirmed the relevance applying it to seaweeds. Indeed, holobionts do not have to be restricted to special processes but should constitute 'a wider vocabulary and framework for host biology in light of the microbiome'.

Few algal models have been studied to date and elucidation of host/microbiome relationships in the case of seaweeds remains to be unravelled (Egan *et al*., 2013; Hollants *et al*., 2013; Florez *et al*., 2017). However, the literature exhibits the crucial role that epibiotic bacterial communities may play in a wide range of ecological interactions, especially via chemicals (Wichard and Beemelmanns, 2018). In particular, the Rhodophyta *Delisea pulchra* has been intensively studied with respect to particular chemically mediated interactions (i.e. quorum sensing modulation via the production of halogenated furanones) between the seaweed and its epibacterial community, including pathogens that can be involved in the temperature-dependent bleaching process (Fernandes *et al*., 2011; Harder *et al*., 2012; Zozaya-Valdes *et al*., 2017). More recently, the role of bacterial communities

associated with the invasive Rhodophyta *Asparagopsis* spp. in southwestern Iberia (Aires *et al*., 2016), the Phaeophyceae *Lobophora* spp. which outcompete corals in New Caledonia (Vieira *et al*., 2016) or crustose coralline algal species that facilitate coral larval settlement (Sneed *et al*., 2015), has also been investigated. Among Phaeophyceae, kelp forests involving Laminariales species exhibit taxonomically diverse bacterial communities in time and space, without a clear relationship to environmental patterns (Michelou *et al*., 2013; Marzinelli *et al*., 2015; Lemay *et al*., 2018). Considering the Phaeophyceae *Ecklonia radiata* in Australia, as for *D. pulchra*, bleaching has been identified as a stronger driver for bacterial communities than environmental parameters such as temperature or light (Marzinelli *et al*., 2015). The surface-associated bacterial communities of the Phaeophyceae *Fucus vesiculosus* from the Western Baltic Sea shores have been found to vary seasonally and be algal species specific (Lachnit *et al*., 2011). In addition, temperature and salinity shifts appear to modify the α-diversity as well as the composition of these bacterial communities (Stratil *et al*., 2013; 2014). Dimethylsulphoniopropionate (DMSP), proline and fucoxanthin, identified at the surface of *F. vesiculosus,* inhibit bacterial attachment (Saha *et al*., 2011; Saha *et al*., 2012) and mainly impact the abundance of surface communities (Lachnit *et al*., 2013). In addition, surface metabolites, including those mediating epibiotic bacterial communities, exhibit seasonal variations related to light and temperature (Saha *et al*., 2014; Rickert *et al*., 2016a).

Conversely, it has also been shown that high phylogenetic variability in bacterial species composition on the Chlorophyta *Ulva australis* was associated with a similar functional composition. These results suggest that the structure of bacterial communities may be addressed at the functional level (Burke *et al*., 2011a,b). In accordance with these findings, different microbial communities have been shown to affect algal growth and development, and morphology of *Ulva intestinalis* and *U. mutabilis* (Spoerner *et al*., 2012; Grueneberg *et al*., 2016; Ghaderiardakani *et al*., 2017). The same research group has more recently demonstrated that DMSP produced by *U. mutabilis* may be used by bacterial strains involved in algal morphogenesis to detect the presence of the alga as a food source (glycerol boundary layer) (Kessler *et al*., 2018).

Taonia atomaria (Woodward) J. Agardh (family Dictyotaceae, class Phaeophyceae, phylum Ochrophyta) is an annual photophilic species of the infralittoral zone, located in calm areas, with a higher abundance in the early summer and very small numbers of individuals from late summer to late winter (Sala and Boudouresque, 1997). This intertidal seaweed, widely reported along the Mediterranean and North-Eastern Atlantic coasts, presents a flat thallus appropriate for surface microbiota investigations. In addition, *T. atomaria* has been previously shown to produce compounds with antifouling properties (Othmani *et al*., 2016a,b). Some of these active molecules, such as sn-3-*O*-(geranylgeranyl)glycerol or (−)-gleenol (Supporting Information Fig. S1), are exuded at its surface and could be involved in the selection of specific epibacterial communities (Othmani *et al*., 2016a,b).

Metabolomics, an emerging approach among the omics sciences, is defined as the qualitative and quantitative analysis of a wide range of metabolites in a biological sample at a specific time (Johnson *et al*., 2016). Its application to specifically determine seaweed surface metabolomes that can originate from both algae and surface microbiota may provide valuable information on their putative interactions.

The aim of this study was to further explore the temporal variations of both the surface metabolome and the epibacterial community of *T. atomaria* in a north-western Mediterranean shore. Thus, a multi-omics analysis was performed to deal with the underlying ecological question about the links between the surface microbiota and the metabolites found at the algal surface, including chemical compounds that could be involved in the defence mechanisms of the host. By coupling meta-omics approaches, new functional insights of biofilm communities can be unravelled, enabling an improved understanding of marine seaweed holobionts.

Results

Monitoring of the surface metabolome of T. atomaria

Thalli of *T. atomaria* were collected in triplicate at the same site from the infratidal zone, each month during the presence of alga from February to July. After the selective extraction of surface compounds using a previously reported specific protocol (Othmani *et al*., 2016a,b), the resulting samples were analysed by LC–MS (See chemical profiles in the Supporting Information Fig. S2). Treatment of the raw MS data with the XCMS package under R environment gave a primary data set with 3065 m/z features and, after data filtering, the final data set was composed of 429 variables (Supporting Information Dataset S1). The PCA score plot for all samples displayed a homogeneous pattern of quality control (QC) samples and blanks, indicating the high stability and repeatability of the analytical instrument (Supporting Information Fig. S3). Taking into account only algal samples, a second PCA score plot was built which clearly indicated an unsupervised clustering of the chemical profiles of surface extracts of *T. atomaria* into three distinct groups: (i) 'winter' (February and March), (ii) 'spring'

(April and May) and (iii) 'summer' (June and July) samples [permutational multivariate analysis of variance (PERMANOVA); $p < 0.05$]. A separation between the 'winter' cluster and the other two clusters were mainly observed on the first component (19.2% of the total variance), while the second component (15.9% of the total variance) allowed the discrimination between 'spring' and 'summer' samples (Fig. 1A).

A second step of this analysis was to build a supervised discriminative model using PLS-DA to determine which surface compounds were implicated in the discrimination between the three groups of samples. In such a model, the variable importance in projection (VIP) score values, commonly used for biomarker selection, indicated the importance of each *m/z* feature in the discrimination between specific sample classes (Supporting Information Fig. S4).

Focus was paid to those variables with a VIP score > 2, corresponding to VIP with scores above the linear regression (Supporting Information Fig. S4B). For each VIP, a molecular formula was proposed based on accurate mass measurement, isotopic patterns and MS/MS data. In most of the cases, a putative identification was proposed (Table 1 and Supporting Information Fig. S5–S22) and for three VIPs (DMSP, proline and proline betaine) the identification was strengthened by the comparison of the data with those of commercial standards. In relation to these results, organization of the whole MS/MS data set using the Global Natural Products Social (GNPS) molecular networking workflow allowed a global view of clusters containing VIPs (Fig. 2) (Wang *et al*., 2016). The main cluster (A) was composed of non-phosphorus betaine lipids identified as diacylglycerylhydroxymethyl-*N*,*N*,*N*-trimethyl-β-alanine (DGTA) derivatives on the basis of the diagnostic fragment ion (*m/z* 236.149, $C_{10}H_{22}NO_5$) for their polar group (Supporting Information Figs. S8, S10, S13 and S18). This class of lipids could be distinguished from the closely related diacylglyceryl-*N*,*N*,*N*-trimethylhomoserines (DGTS) via the absence of a characteristic loss of *m/z* 87 (Roche and Leblond, 2010). This cluster could be divided in two groups constituted by mono-(*lyso*-DGTA) and diacyl (DGTA) derivatives respectively. A second cluster (C) was composed of dipeptides that were putatively characterized using their MS and MS/MS data, and these data were compared with online databases (Supporting Information Figs. S14, S17, S20 and S21).

More than half of the 19 VIPs (Table 1) were amino acids or derivatives, such as dipeptides, and DGTAs. The main part of the VIPs (e.g. proline betaine, DMSP, ceramides and most of the DGTAs) was overexpressed in June and July samples while dipeptides were mostly produced in May and June samples. *Lyso*-DGTA (C20:5) was the only VIP to be more abundant in 'spring' and 'winter' samples than in 'summer' ones.

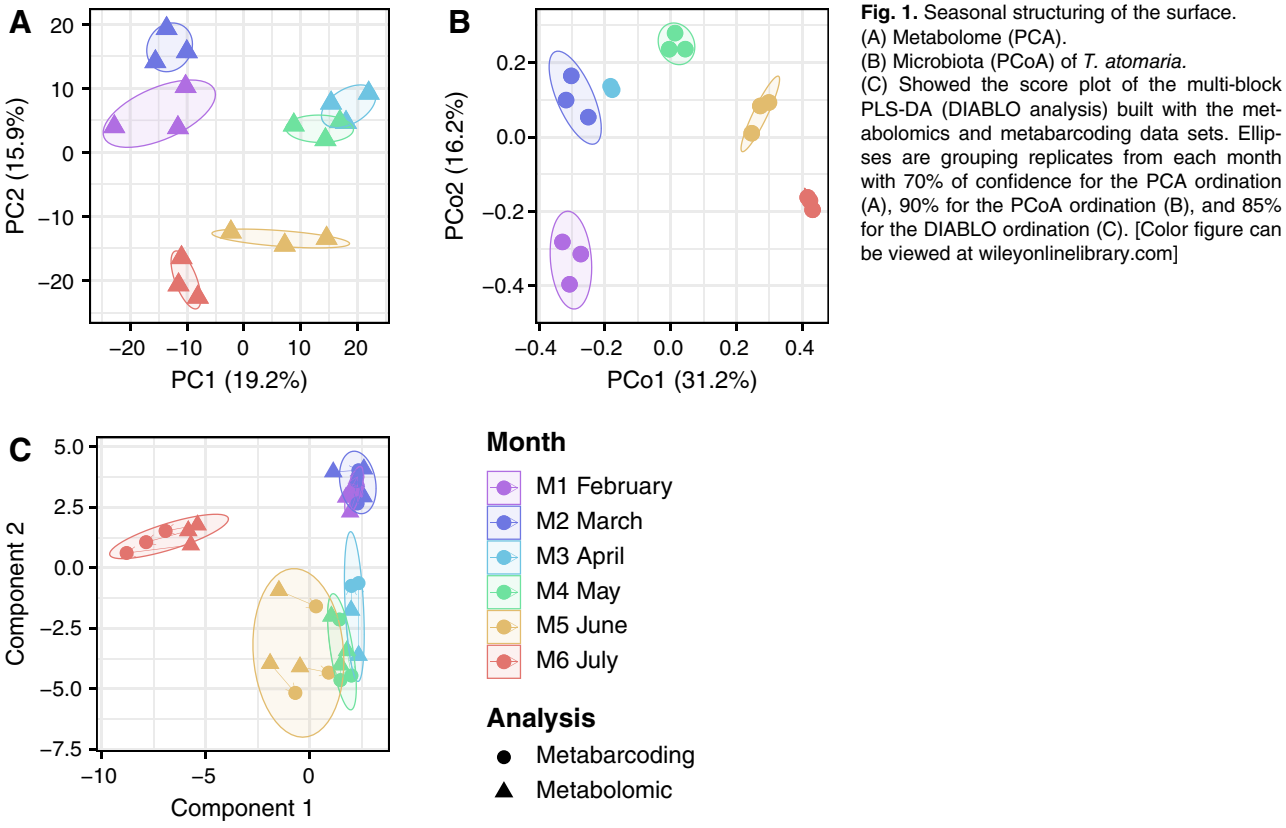

Fig. 1. Seasonal structuring of the surface.
(A) Metabolome (PCA).
(B) Microbiota (PCoA) of *T. atomaria.*
(C) Showed the score plot of the multi-block PLS-DA (DIABLO analysis) built with the metabolomics and metabarcoding data sets. Ellipses are grouping replicates from each month with 70% of confidence for the PCA ordination (A), 90% for the PCoA ordination (B), and 85% for the DIABLO ordination (C). [Color figure can be viewed at wileyonlinelibrary.com]

Table 1. List of the biomarkers (VIP score ≥ 2) identified by LC–HRMS for the seasonal discrimination of the surface extracts of *T. atomaria*. [Color table can be viewed at wileyonlinelibrary.com]

VIP N°	*m/z*	RT (s)	VIP score	Formula	Mass error (ppm)	mσ[a]	MS/MS fragment ions (relative abundance in %)	Putative identification[b]	Feb.	Mar.	Apr.	May	Jun.	Jul.	Colour code[c]
1	144.1018	55	4.3	$C_7H_{14}NO_2$	0.5	4.5	144.1018 $[M + H]^+$ (100), 102.0548 $[C_4H_8NO_2]^+$ (2), 84.0807 $[C_5H_{10}N]^+$ (25), 58.0650 $[C_3H_8N]^+$ (19)	Proline betaine[d]							3
2	135.0473	53	3.2	$C_5H_{11}O_2S$	0.8	4.5	135.0473 $[M + H]^+$ (25), 73.0282 $[C_3H_5O_2]^+$ (100), 63.0261 $[C_2H_7S]^+$ (92), 61.0104 $[C_2H_5S]^+$ (4), 55.0177 $[C_3H_3O]^+$ (8)	DMSP[d]							2.5
3	538.5195	710	3.1	$C_{34}H_{68}NO_3$	−0.3	5.5	520.5096 $[M - H_2O + H]^+$ (2), 502.4972 $[M - 2 H_2O + H]^+$ (1), 282.2794 $[M - H_2O - C_{16}H_{30}O + H]^+$ (21), 264.2687 $[M - 2 H_2O - C_{16}H_{30}O + H]^+$ (100), 252.2688 $[C_{17}H_{34}N]^+$ (12)	Ceramide (dC18:1/C16:0)							0
4	860.6397	700	3.1	$C_{54}H_{86}NO_7$	0.6	19.7	860.6397 $[M + H]^+$ (100), 550.4108 $[M - C_{22}H_{30}O + H]^+$ (13), 548.3949 $[M - C_{22}H_{32}O + H]^+$ (22), 546.3791 $[M - C_{22}H_{34}O + H]^+$ (13), 236.1506 $[C_{10}H_{22}NO_5]^+$ (5)	DGTA (C44:10)							−2.5
5	116.0706	51	2.9	$C_5H_{10}NO_2$	−0.3	3.4	116.0706 $[M + H]^+$ (2), 70.0652 $[M - HCO_2H + H]^+$ (100)	Proline[d]							−5
6	856.6093	679	2.8	$C_{54}H_{82}NO_7$	−0.8	4.2	856.6093 $[M + H]^+$ (100), 546.3791 $[M - C_{22}H_{30}O + H]^+$ (67), 528.3690 $[M - C_{22}H_{30}O - H_2O + H]^+$ (11), 236.1491 $[M - 2 C_{22}H_{30}O + H]^+$ (7)	DGTA (C22:6/C22:6)							
7	201.1637	689	2.8	$C_{15}H_{21}$	0.6	18.4	159.1167 $[C_{12}H_{15}]^+$ (29), 145.1012 $[C_{11}H_{13}]^+$ (100), 131.0856 $[C_{10}H_{11}]^+$ (9), 105.0697 $[C_8H_9]^+$ (10), 57.0697 $[C_4H_9]^+$ (7)	Sesquiterpene IV							
8	324.3260	649	2.8	$C_{21}H_{42}NO$	−2.0	3.4	324.3260 $[M + H]^+$ (100), 306.3157 $[M - H_2O + H]^+$ (5), 284.2947 $[C_{18}H_{38}NO]^+$ (20), 282.3161 $[C_{19}H_{40}N]^+$ (10), 110.0973 $[C_7H_{12}N]^+$ (18), 84.0808 $[C_5H_{10}N]^+$ (12)	$C_{21}H_{41}NO$							
9	520.3630	489	2.7	$C_{30}H_{50}NO_6$	−1.5	6.7	520.3630 $[M + H]^+$ (100), 236.1492 $[M - C_{20}H_{28}O + H]^+$ (4)	*Lyso*-DGTA (C20:5)							
10	246.1447	62	2.6	$C_{10}H_{20}N_3O_4$	1.0	1.5	228.1341 $[M - H_2O + H]^+$ (32), 183.1125 $[C_9H_{15}N_2O_2]^+$ (45), 138.0910 $[C_8H_{12}NO^+]^+$ (5), 118.0862 $[C_5H_{12}NO_2]^+$ (26), 101.0710 $[C_4H_9N_2O^+]^+$ (8), 84.0444 $[C_4H_6NO]^+$ (100), 83.0602 $[C_4H_7N_2]^+$ (60), 72.0807 $[C_4H_{10}N]^+$ (69)	Gln-Val							
11	741.6140	621	2.5	$C_{44}H_{86}O_6P$	2.2	9.4	601.5197 $[C_{39}H_{69}O_4]^+$ (100), 445.2961 $[C_{27}H_{41}O_5]^+$ (30), 339.2889 $[C_{21}H_{39}O_3]^+$ (39), 184.0735 $[C_5H_{11}O_4P + NH_4^+]^+$ (84)	n.d.[e]							
12	510.4886	694	2.5	$C_{32}H_{64}NO_3$	−0.9	11.2	492.4776 $[M - H_2O + H]^+$ (2), 474.4672 $[M - 2 H_2O + H]^+$ (1), 282.2792 $[M - H_2O - C_{14}H_{26}O + H]^+$ (22), 264.2686 $[M - 2 H_2O - C_{14}H_{26}O + H]^+$ (100), 252.2686 $[C_{17}H_{34}N]^+$ (15)	Ceramide (dC18:1/C14:0)							

(Continues)

Table 1. Continued

VIP N°	*m/z*	RT (s)	VIP score	Formula	Mass error (ppm)	mσ[a]	MS/MS fragment ions (relative abundance in %)	Putative identification[b]	Feb.	Mar.	Apr.	May	Jun.	Jul.	Colour code[c]
13	260.1605	77	2.4	$C_{11}H_{22}N_3O_4$	−0.2	12.3	242.1498 $[M - H_2O + H]^+$ (29), 197.1283 $[C_{10}H_{17}N_2O_2]^+$ (27), 196.1449 $[C_{10}H_{18}N_3O]^+$ (16), 132.1016 $[C_6H_{14}NO_2^{+}]^+$ (20), 129.0659 $[C_5H_9N_2O_2]^+$ (11), 101.0709 $[C_4H_9N_2O]^+$ (8), 86.0964 $[C_5H_{12}N]^+$ (84), 84.0443 $[C_4H_6NO]^+$ (100), 83.0602 $[C_4H_7N_2]^+$ (59)	Gln-Leu[f]							
14	708.5776	695	2.4	$C_{42}H_{78}NO_7$	−0,5	11.1	708.5776 $[M + H]^+$ (100), 498.3782 $[M - C_{14}H_{26}O + H]^+$ (7), 472.3629 $[M - C_{16}H_{28}O + H]^+$ (21), 446.3474 $[M - C_{18}H_{30}O + H]^+$ (20), 236.1495 $[C_{10}H_{22}NO_5]^+$ (5)	DGTA (C32:2)							
15	583.4353	659	2.3	$C_{37}H_{59}O_5$	0.7	12.7	583.4353 $[M + H]^+$ (26), 565.4250 $[M - H_2O + H]^+$ (5), 335.2585 $[C_{21}H_{35}O_3]^+$ (100), 305.2111 $[C_{19}H_{29}O_3]^+$ (16), 261.2213 $[C_{18}H_{29}O]^+$ (13), 231.1743 $[C_{16}H_{23}O]^+$ (38), 81.0698 $[C_6H_9]^+$ (52)	DAG (C18:3/C16:4)							
16	294.1444	126	2.3	$C_{14}H_{20}N_3O_4$	−0.0	4.6	276.1350 $[M - H_2O + H]^+$ (28), 231.1120 $[C_{13}H_{15}N_2O_2]^+$ (19), 166.0865 $[C_9H_{12}NO_2]^+$ (57), 120.0807 $[C_8H_{10}N]^+$ (100), 101.0712 $[C_4H_9N_2O]^+$ (10), 84.0446 $[C_4H_6NO]^+$ (64), 83.0599 $[C_4H_7N_2]^+$ (63)	Gln-Phe							
17	229.1182	162	2.1	$C_{10}H_{17}N_2O_4$	0.4	2.9	183.1124 $[C_9H_{15}N_2O_2]^+$ (11), 118.0863 $[C_5H_{12}NO_2]^+$ (14), 84.0444 $[C_4H_6NO]^+$ (100), 72.0806 $[C_4H_{10}N]^+$ (78)	Gln-Val derived dipeptide							
18	331.0116	99	2.0	$C_{12}H_{11}O_9S$	0.7	9.6	251.0550 $[M - SO_3 + H]^+$ (57), 233.0451 $[M - SO_3 - H_2O + H]^+$ (70), 209.0445 $[C_{10}H_9O_5]^+$ (23), 205.0501 $[C_{11}H_9O_4]^+$ (23), 191.0333 $[C_{10}H_7O_4]^+$ (17), 165.0544 $[C_9H_9O_3]^+$ (50), 163.0395 $[C_9H_7O_3]^+$ (35), 139.0391 $[C_7H_7O_3]^+$ (100)	Difucol-*O*-sulfate							

a. Constructor statistical match factor (comparison of theoretical and experimental isotopic patterns).
b. Abbreviations: DAG: diacylglycerol; DGTA: diacylglycerylhydroxymethyl-*N*,*N*,*N*-trimethyl-*β*-alanine; DMSP: dimethylsulfoniopropionate; Gln: glutamine; Ile: isoleucine; Leu: leucine; Phe: phenylalanine; Val: valine.
c. Colour codes represented mean normalized concentration values.
d. These identifications were confirmed with commercial standards.
e. Not determined.
f. Not distinguishable from Gln-Ile.

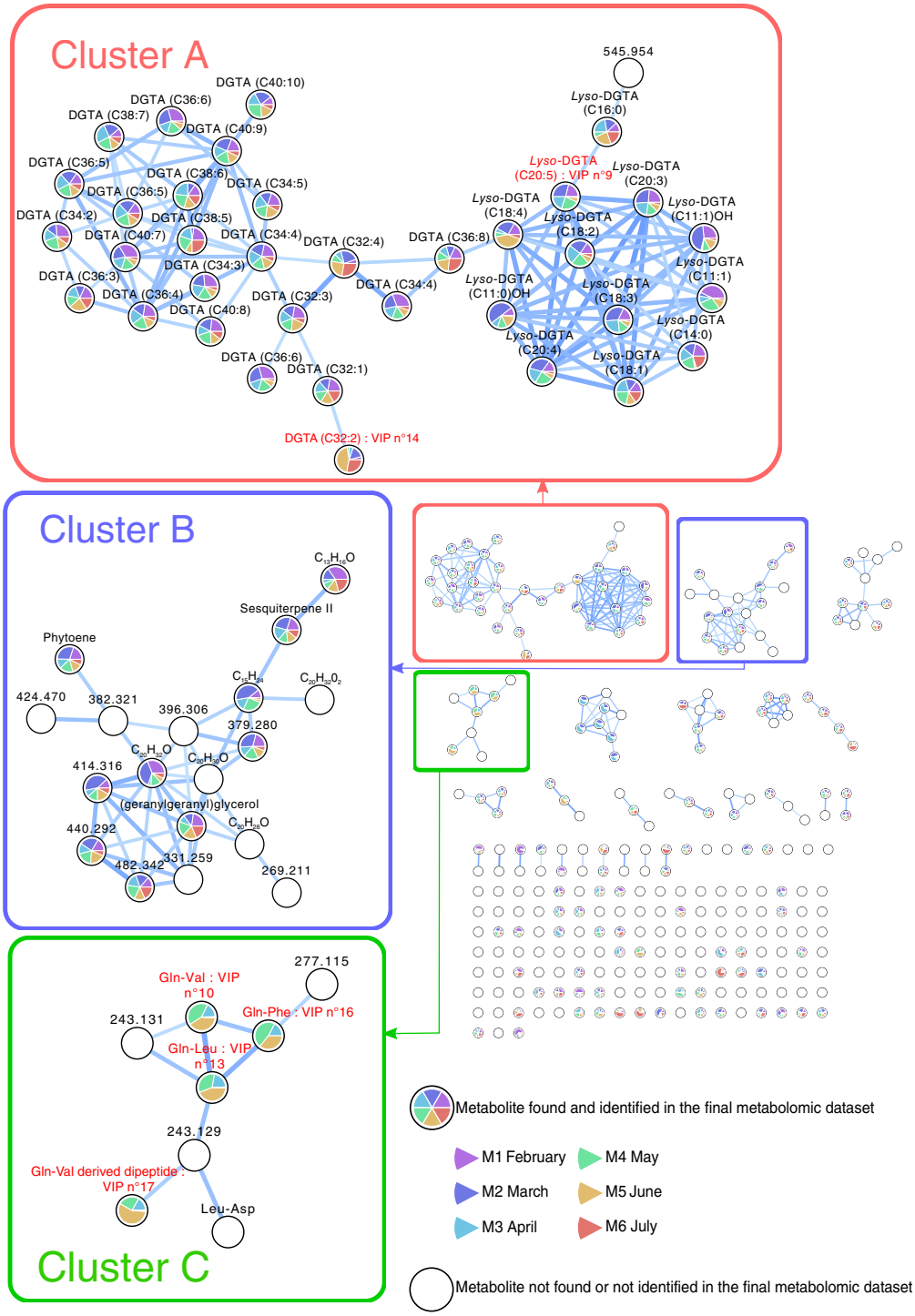

Fig. 2. Molecular network of HRMS fragmentation data obtained from surface extracts of *T. atomaria* (collected monthly from February to July). [Color figure can be viewed at wileyonlinelibrary.com]

In addition, attention was focused on annotated compounds [compounds previously detected at the surface of the thalli of *T. atomaria* (Othmani *et al*., 2016a,b) or already studied in previous ecological studies (e.g. fucoxanthin, mannitol)], in order to evaluate their temporal fluctuations (Fig. 3). The biosynthesis of fucoxanthin, geranylgeranylglycerol and sesquiterpenes I, II and V was fairly constant during the survey ($p > 0.05$), while those of mannitol showed a slight decline during summer ($p < 0.05$). Despite significant differences ($p < 0.05$), samples collected in winter and summer exhibited the highest amounts of sesquiterpene III. Finally, proline, DMSP and

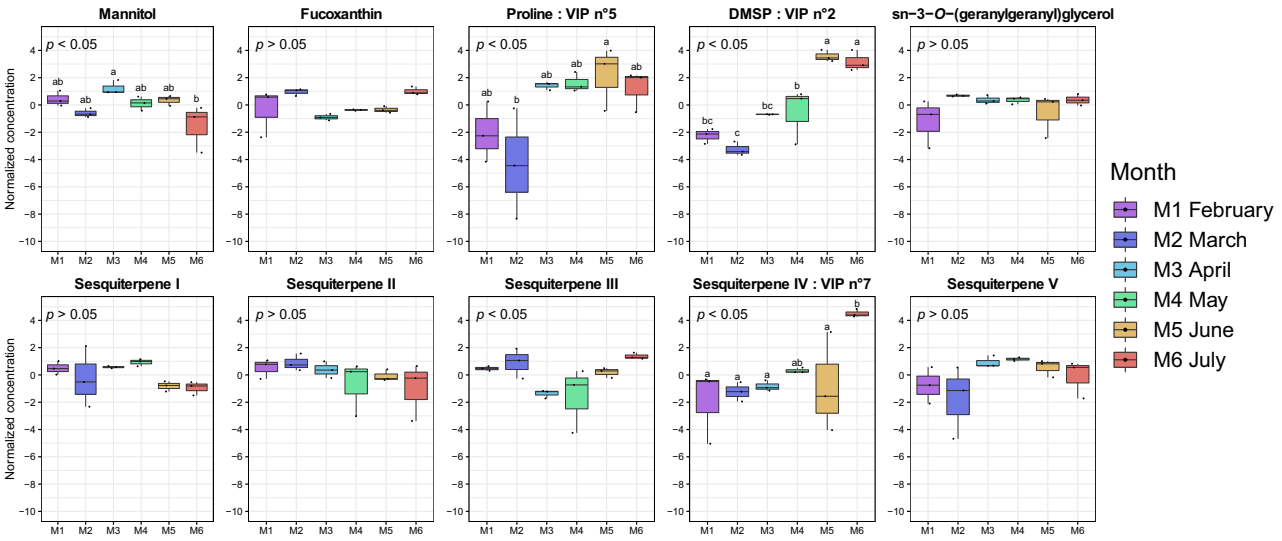

Fig. 3. Seasonal variations of some selected surface metabolites of *T. atomaria*. Individual metabolites obtained after UPLC–MS analysis were normalized by the sum, log10-transformed and mean-centred. A one-way ANOVA followed by post hoc tests (HSD) allowed to show significant variations for relative concentrations of each metabolite during the year. [Color figure can be viewed at wileyonlinelibrary.com]

sesquiterpene IV were more present at the algal surface in summer than in the winter, with the highest production level being reached in June for proline (VIP n°1), in June and July for DMSP (VIP n°2) and in July for sesquiterpene IV (VIP n°7) ($p < 0.05$). Moreover, with the aim of determining how the richness of the chemical production of *T. atomaria* varied according to season, an estimate of the algal chemodiversity was determined using the Shannon index (Fig. 4A). The algal chemodiversity increased significantly from March to July ($p < 0.05$).

16S rDNA gene-based analysis of epibiotic bacterial communities of T. atomaria

The 16S rDNA gene was amplified and sequenced for three thalli replicates for each month from February to July. In total, 1,556,091 sequences and 63,494 OTUs were obtained with the Illumina MiSeq sequencing. Samples were rarefied to the lowest number of sequences, i.e. 11,469. One sample collected in April was removed from the analysis due to DNA contamination. α-diversity indexes indicated highly diversified communities with a significant trend observed for the Simpson index by decreasing from February to April before increasing from April to July ($p < 0.05$) (Fig. 4B–D).

The PCoA based on Bray–Curtis dissimilarity distances (Fig. 1B) showed a high similarity between bacterial communities described from algal samples collected in the same month, together with a shift of these communities with time (PERMANOVA, $p < 0.05$). At the class level (Supporting Information Fig. S23), α- and γ-proteobacteria dominated the communities without

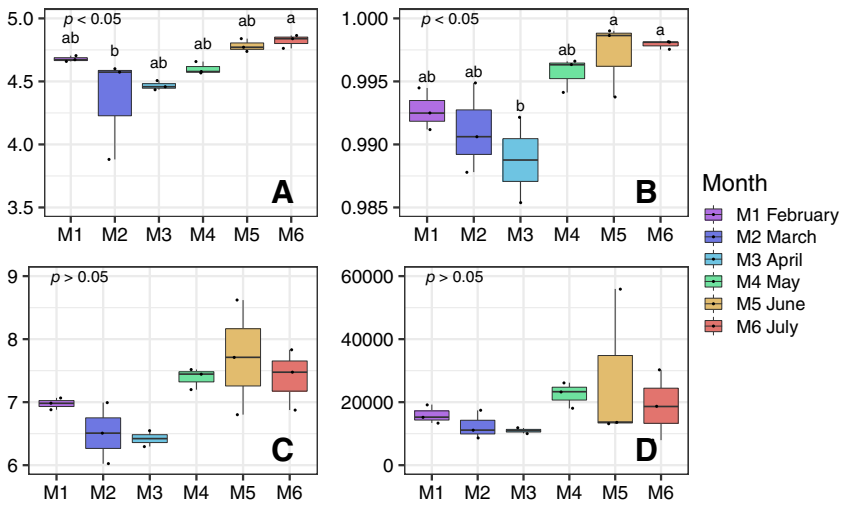

Fig. 4. Seasonal dynamics of diversity indexes.
(A) The chemodiversity measures calculated using Shannon index with the metabolomics dataset.
(B, C and D) The epibacterial alpha-diversity measures, respectively, calculated using Simpson, Shannon and Chao1 indexes with the 16S metabarcoding data set. A one-way ANOVA followed by post hoc tests (HSD) allowed to show significant variations for the indexes during the year. [Color figure can be viewed at wileyonlinelibrary.com]

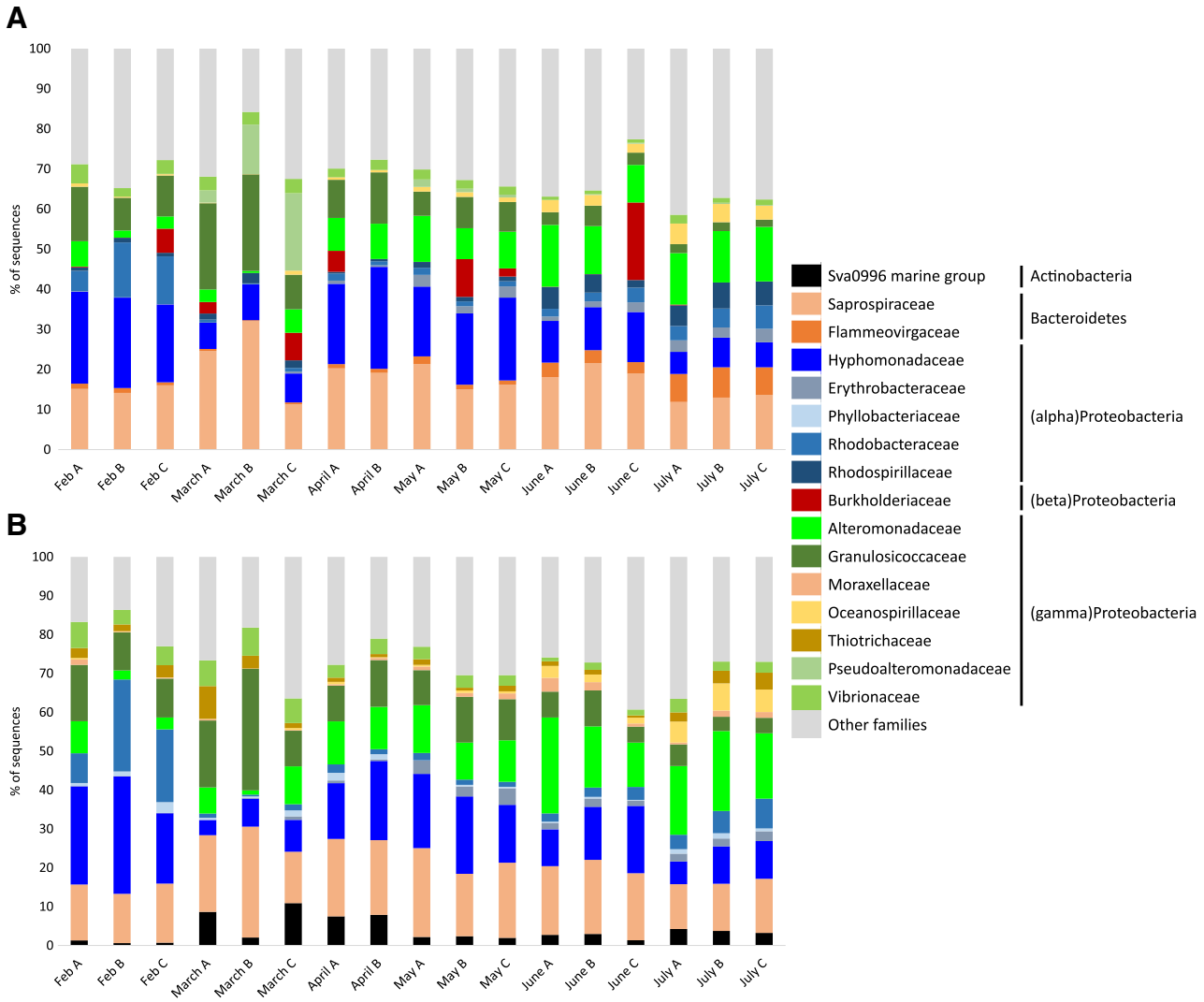

Fig. 5. Seasonal variations of the epibacterial communities on *T. atomaria* at the family level (A: total community, B: core community). A, B, C in sample names represent biological replicates. % in B are % of all the core sequences. [Color figure can be viewed at wileyonlinelibrary.com]

significant seasonal change, except for a higher dominance of the α-proteobacteria in February (reaching 69% of the OTUs for the whole community) and an increase of the relative abundance of the *Cytophagia* (Bacteroidetes) in June and July. Flavobacteria, Sphingobacteria and unidentified Bacteroidetes, in addition to *Cytophagia*, accounted for 19–37% of the communities. Actinobacteria altogether never exceeded 12%, whereas β- and δ-proteobacteria showed high variations, sometimes reaching high percentages (such as 25% in June for β-proteobacteria). At the family level (Fig. 5A), the dominant taxa were Saprospiraceae (Bacteroidetes), Hyphomonadaceae (α-proteobacteria), Granulosicoccaceae (exclusively the genus *Granulosicoccus*) and Alteromonadaceae (γ-proteobacteria), representing together between 33% and 56% of all sequences during the survey. Seasonal trends could be observed with the dominance, when the alga appeared in winter, of Saprospiraceae, Hyphomonadaceae, Rhodobacteraceae (mainly reported as unidentified) and Granulosicoccaceae, together with Vibrionaceae. The latter included at least 80% of *Vibrio* spp. with an increasing number of *Photobacterium* spp. in the spring and summer. Pseudoalteromonadaceae (exclusively *Pseudoalteromonas* spp.) could only be observed in March. During spring and summer, Alteromonadaceae (mainly the BD1-7 clade, which belongs to the oligotrophic marine γ-proteobacteria, OMG) clearly replaced Granulosicoccaceae as the dominant γ-proteobacteria, and an increase in Oceanospirillaceae was observed. α-proteobacteria appeared to diversify with the decrease in Hyphomonadaceae and Rhodobacteraceae that occurred concomitantly with the increase in Erythrobacteraceae (all the time around 70% of *Erythrobacter* spp.) and Rhodospirillaceae (mainly reported as unidentified taxa). Flammeovirgaceae also increased

from May to July. Finally, among the Saprospiraceae, which remained constant during the survey, members of the genus *Lewinella* significantly increased while, on the contrary, *Aureispira* spp. decreased.

The core OTUs were defined as OTUs observed in at least one replicate each month. Thus, 1,544 OTUs, i.e. between 11% and 21% of the total OTUs per month, constituted the epibacterial core community of *T. atomaria* from February to July (Supporting Information Fig. S24). This core community corresponded to significantly higher percentages of sequences than OTUs for each sample, ranging from 27% to 53% ($p < 0.05$). As these percentages of sequences appeared higher than the percentages of OTUs for the corresponding samples, this suggested that the core was not only composed by rare OTUs. In addition, a significant decrease in the percentage of the total core community sequences could be noticed from April to July ($p < 0.05$), without any significant variation in the percentage of OTUs. Similar trends as for the overall community could be noticed for the core community at the family level (Fig. 5B). In particular, the four dominant groups (>10%) remained the same (Saprospiraceae, Hyphomonadaceae, Granulosicoccaceae and Alteromonadaceae), together with the seasonal shift among γ-proteobacteria (and the replacement of Granulosicoccaceae by Alteromonadaceae), the significant presence of Rhodobacteraceae only in February or the occurrence of Oceanospirillaceae and Erythrobacteraceae as the sub-dominant groups in the summer (1–10%). However, the Sva0996 marine group (Actinobacteria) and Moraxellaceae (γ-proteobacteria) specifically appeared in the core community as dominant and sub-dominant respectively. The increase in Alteromonadaceae in the core community in spring and summer could be directly associated with the increase in members of the BD1-7 clade: they reached between 52% and 80% of the Alteromonadaceae in the core community, while they ranged between 22% and 46% in the overall community. Similarly, when identified, one genus clearly dominated each family in the core community (e.g. *Granulosicoccus* for Granulosicoccaceae, *Robiginitomaculum* for Hyphomonadaceae, *Erythrobacter* for Erythrobacteraceae, *Balneathrix* for Oceanospirillaceae, and *Thiothrix* for Thiotrichaceae).

Multi-omics approach to assess temporal variations of T. atomaria

A multi-block PLS-DA model was built using the MixOmic DIABLO analysis with the metabolomics and metabarcoding data sets. The resulting score plot (Fig. 1C) showed an initial strong seasonal co-variation between epibacterial communities and surface metabolites, with a correlation coefficient of 0.95 between the two data sets. This trend was confirmed by a Mantel test ($p < 0.01$). The second component progressively discriminated samples collected in February and March from those obtained in April and May. Samples from April to July were then progressively discriminated along the first component. Similar results can be observed on the heatmap of the relative abundance of a panel of highly relevant variables selected from the supervised multi-block PLS-DA model (Supporting Information Fig. S25). Three groups of samples were clearly distinct within the dendrogram: February and March, then April, May and June, and finally samples collected in July. The relative abundance of the selected variables on the heatmap representation showed then a continuous covariation of surface metabolites and epibacterial OTUs from February to July.

Two clusters were observed on the correlation network built with the 108 most discriminant variables highlighted by the multi-block PLS-DA, among the surface metabolites and epibacterial OTUs data sets (Fig. 6). The first cluster, on the top, showed mainly metabolites and epibacterial OTUs which were positively correlated due to their high relative abundance during the 'spring period' (April, May and June). Interestingly, almost half of these OTUs were affiliated with the same group (BD1-7 clade, Alteromonadaceae), while annotated metabolites were proline and dipeptides. This cluster also showed a few unidentified metabolites that were negatively correlated to these specific OTUs. The second cluster, on the bottom, revealed mainly positive correlations between several metabolites and OTUs which were both abundant during the 'summer period' (June and July). The metabolites involved in such relationships were mostly non-polar lipids such as a ceramide, a di-(DAG) and a triacylglycerol (TAG) but also DMSP, proline betaine and sesquiterpene IV. Among the related OTUs, Erythrobacteraceae, Flammeovirgaceae, Oceanospirillaceae and Rhodospirillaceae were the main families. Interestingly, several DGTAs and *lyso*-DGTAs were negatively correlated with these 'summer epibacterial OTUs', showing lower relative concentrations during the 'summer period'.

Discussion

Holobionts put seaweed studies in the context of an integrated social unit as it was clearly observed that algal phenotypes are deeply affected by their complex surface-associated microbial communities. For example, bleaching of the Australian Rhodophyta *D. pulchra* (Fernandes *et al*., 2012; Zozaya-Valdes *et al*., 2017) or Ochrophyta kelps (Marzinelli *et al*., 2015) was associated with a shift in the algal epibacterial community structure associated with the lack of production of quorum sensing inhibitors (halogenated furanones) by the algal host. The Phaeophyceae *Ecklonia radiata* (kelp) maintains more specific microbial communities than those found its immediate surroundings but when the alga becomes

stressed and bleaches, this specificity breaks down (Marzinelli *et al*., 2015). The cellular differentiation of Chlorophyceae (*Ulva* spp.) was shown to be associated with thalusin production by host-associated bacteria (Matsuo *et al*., 2005). Within the framework of complex relationships, coral larvae may be able to use the observed differences in bacterial community composition on crustose coralline algal species to assess the suitability of these substrata for settlement and selectively settle on algal surfaces that bear beneficial bacteria (Sneed *et al*., 2015). This also indicates that host conditions could more strongly influence bacterial communities than geographical and environment-related parameters.

Diversity and composition of total and core microbiota associated with the surface of T. atomaria

This study aimed to identify the diversity and the composition of the epibacterial communities of the Dictyotaceae *T. atomaria* collected on the French Mediterranean coast and to unravel the seasonal variation of these microbiota in relation to those of surface metabolomes. Seaweeds and their surface-associated microbiota are considered as holobionts (Egan *et al*., 2013).

Highly diversified bacterial communities with the co-dominance of α-, γ-proteobacteria and Bacteroidetes colonized *T. atomaria* surfaces. The structure of these communities was similar to those of typical biofilms described on other seaweeds or artificial surfaces (Wahl *et al*., 2012; Dang and Lovell, 2016). A marked seasonal trait occurred in this colonization process, which involved pioneer bacterial taxa (r-strategists especially among Rhodobacteraceae and Alteromonadaceae) followed by more adapted and seaweed-specific ones (K-strategists). Increasing seawater temperature and associated irradiation (data not shown) would be involved in the shaping of the epibacterial communities from February (winter) to July (summer). The concept of core community, still poorly studied in marine ecosystems, is related to the stable part of the bacterial community (Astudillo-García *et al*., 2017). The core is generally defined on the basis of a minimal percentage of occurrence in studied samples. Nevertheless, the choice of this abundance threshold is questionable. We consequently decided to define the core community not using an abundance threshold but as the set of OTUs identified all the months in at least one replicate whatever their abundance. Especially, this definition allowed to exclude OTUs not detected one specific month. Using this definition, the core community already included between 30% and 60% of the sequences. A more stringent definition would have increased this percentage and we assumed that one of the interest of the core concept is to focus on a more specific part of the microbial community. The core community of *T. atomaria* accounted for a large part of the whole set of sequences during the study, but this finding was not observed when considering OTUs. Thus, few dominating abundant OTUs together with several transient low abundant OTUs seem to characterize the core community. The core community showed a similar composition as the overall community at the family level, but a lower diversity at the genus level. In addition, two original taxa (Sva0996 marine group and *Thiothrix* spp) emerged in the core community of *T. atomaria.* Members of Sva0996 marine group are Gram-positive Actinobacteria that remain largely unknown. These bacteria were only sporadically noticed in various marine environments such as sediment surfaces of the Arctic ocean (Li *et al*., 2009), enriched bacterioplankton during phytoplankton blooms in the Sargasso Sea (Nelson *et al*., 2014) or associated with sponges (Verhoeven *et al*., 2017). *Thiothrix* spp. belong to the filamentous sulphur-oxidizing bacteria, which have been mainly reported from activated-sludge wastewater treatment plants or as ectosymbionts of marine (Gillan and Dubilier, 2004) or freshwater (Flot *et al*., 2014) amphipods. However, the latter bacteria were also reported to form white-coloured films on portions of the surface of aquatic macrophytes located within the hydrothermal flow of vents of Yellowstone Lake (Konkol *et al*., 2010). *Thiothrix* spp., as a sulphide oxidiser, was thus suggested to be, in part, responsible for limitation of the toxicity associated with high sulphide concentrations. However, the poorly diversified dense mats dominated by *Thiothrix* spp. could also limit the photosynthesis of the macrophytes. No mats were observed at the surface of *T. atomaria* and considering its sulphur metabolism, the occurrence of these taxa remained difficult to interpret.

Signalling cyclic dipeptides associated with the OMG BD1-7 clade

Multi-block analyses and correlation networks between the most discriminant metabolites and bacterial OTUs at the surface of *T. atomaria* in their respective seasonal clustering confirmed the similar seasonal dynamic but mostly highlighted their putative interactions. The first cluster of the correlation network (Fig. 6) exhibited both OTUs and metabolites which were more abundant in the spring and positively correlated to each other. Most of the corresponding taxa were related to Alteromonadaceae, especially members of the BD1-7 clade which have been previously reported as pioneer bacteria on marine surfaces (Dang and Lovell, 2016; Pollet *et al*., 2018) and in nutrient-depleted environments (Spring *et al*., 2015). If already identified in the low nutrients containing Mediterranean Sea, the BD1-7 clade was not reported as a

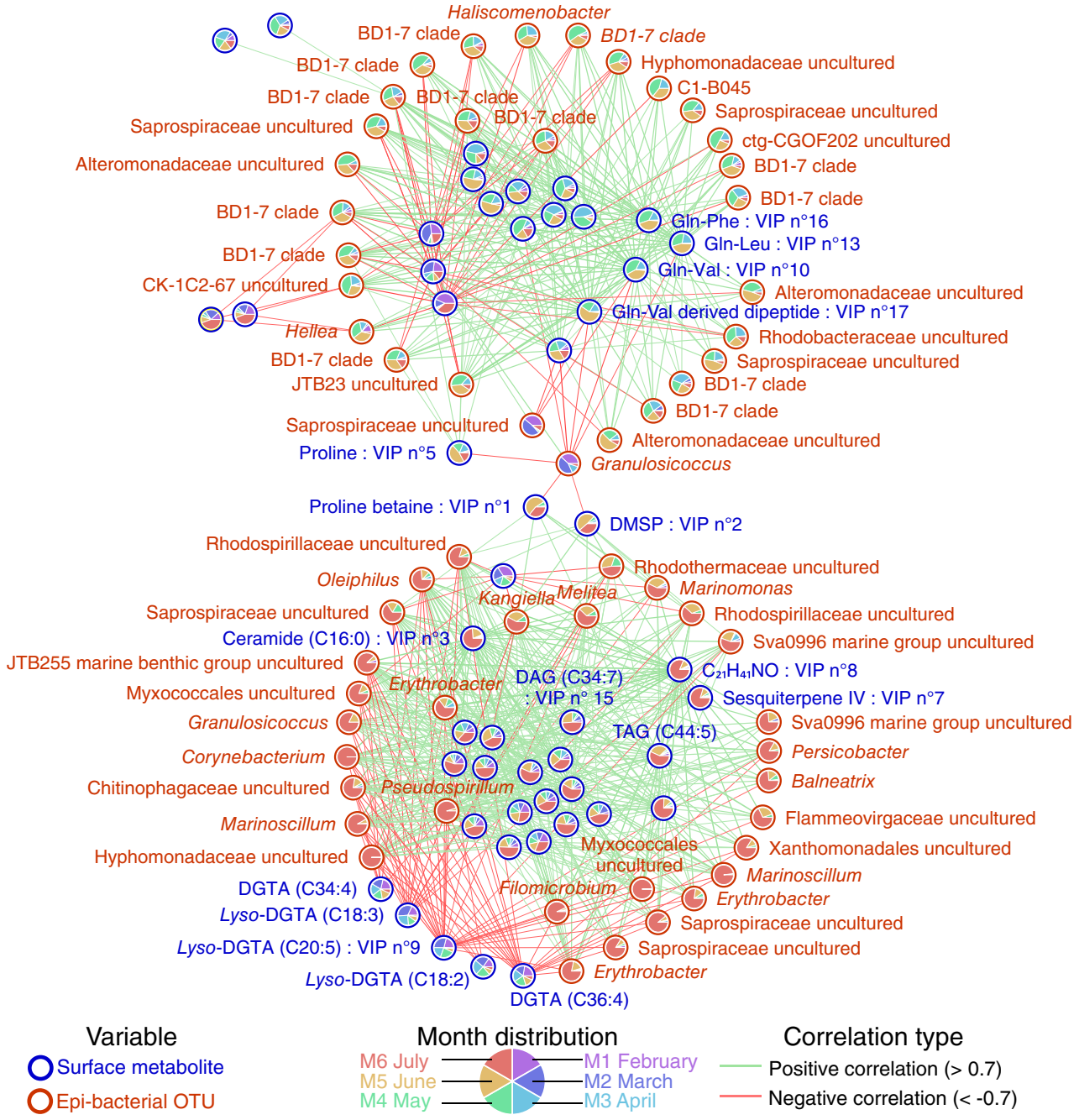

Fig. 6. Seasonal correlation network (multi-block PLS-DA) of the surface metabolome and the epibacterial communities of *T. atomaria.* Discriminant OTUs (orange circles and names) and metabolites (blue circles and names) are positively (green) or negatively (red) connected. Seasonal variation of their relative occurrence during the year was also represented inside the circles with pie charts. [Color figure can be viewed at wileyonlinelibrary.com]

major taxon of biofilms formed on artificial substrates in the vicinity of the collection site (Briand *et al*., 2017), indicating a potential specific selection by *T. atomaria.* In addition, as a major component of the core community that represented a significant part of the total surface community, this clade should play a major ecological role. Most of the related metabolites identified at the surface of the alga were cyclic dipeptides: such compounds have been widely reported from bacteria and showed diverse biological activities (e.g. antimicrobial, antioxidant, antiviral or antitumor) (Huang *et al*., 2010). It was suggested that cyclic dipeptides could play a role in bacterial and trans-kingdom signalling (Ortiz-Castro *et al*., 2011).

DMSP and proline betaine exhibited a key role within the correlation network

On the correlation network built with discriminant variables of the surface metabolome and the microbiota of *T. atomaria* (Fig. 6), the link between the two clusters rests on the genus *Granulosicoccus.* The latter has been identified as a psychrotrophic taxon, widely reported from Antarctic coastal seawaters (Baek *et al*., 2014) and sediments (Wang *et al*., 2017) but also from the surface of an unidentified brown alga (Park *et al*., 2014) or the Mediterranean Chlorophyceae *Caulerpa* spp. (Rizzo *et al*., 2016). This major node of the network was negatively related to the two most important VIPs for the metabolite clustering, i.e. DMSP and proline betaine (*N*,*N*-dimethylproline also known as stachydrine). Proline betaine and DMSP and, to a lesser extent, proline, were found to be the main discriminant surface metabolites for differentiation between months. The levels of these compounds constantly increased from February to June (Table 1 and Fig. 3). These low molecular mass molecules belong to a family of compounds that are collectively termed 'compatible solutes' and accumulated to high intracellular concentrations in a wide range of organisms (McNeil *et al*., 1999). In addition to their firmly established osmoprotective function, various physiological and ecological roles have been demonstrated for these compounds (e.g. stabilization of proteins and membranes, protection of photosystem II, supply of carbon and nitrogen). More broadly, compatibles solutes have been shown to participate to the acclimation of organisms to a number of stresses. In the particular case of algae, proline and DMSP have been detected at the surface of the brown alga *F. vesiculosus* and it has been demonstrated that these compounds had antibacterial properties at natural concentrations (Saha *et al*., 2012). More particularly, DMSP content was high at 20°C and then decreased at 25°C and was globally higher under dark conditions (Saha *et al*., 2014). In previous works dealing with total extracts of several macroalgae, it has been demonstrated that DMSP content increased with irradiance and decreased with temperature, with such variations being in accordance with the roles of DMSP as an antioxidant or cryoprotectant (Karsten *et al*., 1992; Lyons *et al*., 2010). More recently, a study has shown that DMSP released by the Chlorophyta *U. mutabilis* also acted as a chemoattractant for *Roseovarius* sp., a bacterium known to induce the morphogenesis of *Ulva* (Kessler *et al*., 2017). In the case of proline, the effect of temperature and light on its surface concentration on *F. vesiculosus* was shown to be limited (Saha *et al*., 2014), while an increase in proline levels was observed in the red alga *Gracilaria tenuistipitata* exposed to high temperatures (e.g. Chang and Lee, 1999).

In this study, DMSP, proline and proline betaine contents reached their maximal values in June and, to a lesser extent, in July when irradiance, sea temperature and fouling pressure were high. Their slight decrease in July coincided with the appearance of bleached portions on thalli of *T. atomaria.* This could thus explain such a trend which was previously reported for DMSP in the green alga *Codium fragile* (Lyons *et al*., 2010). Kessler *et al*. (2017) demonstrated that bacteria essential for *U. mutabilis* were able to catabolize algal DMSP into methanethiol and dimethylsuphide (DMS) faster than *de novo* production by the algal host in order to prevent the attraction of additional bacteria. Nevertheless, in the present work, algal samples collected *in situ* bore a complex bacterial community which certainly induced more complex chemically based relationships that those described by an *in vitro* tripartite model. Moreover, it cannot be excluded that DMSP found in the samples was also produced by microorganisms associated at the surface of *T. atomaria.*

Interestingly, mannitol which has also been suspected to be implicated in algal response to stress (Dittami *et al*., 2011) remained constant from February to June and declined sharply in July (Fig. 3). This storage compound has previously been used as a proxy for energy availability in order to produce chemical defences, and its production has been negatively correlated to microfouling colonization (Rickert *et al*., 2015; Rickert *et al*., 2016b)

What about the role of the key network compounds DGTAs?

The second cluster at the bottom of the correlation network (Fig. 6) illustrated the higher diversity of summer surface microbiotea. Some of the taxa were major representatives of the core microbiota, e.g. *Balneathrix*, *Erythrobacter* and especially the Sva0996 marine group. *Erythrobacter* spp. are marine ubiquitous aerobic anoxygenic phototrophic bacteria, which have already been reported as the major taxa of biofilm communities on artificial surfaces (Briand *et al*., 2017; Oberbeckmann *et al*., 2018). As cyanobacteria failed to be identified in the surface community of *T. atomaria*, *Erythrobacter* spp. could be major actors of the primary production at the algal surface.

OTUs from this cluster were negatively correlated with several DGTAs. These non-phosphorus-containing betaine lipids were assumed to have similar functions to phospholipids and replaced this class of polar lipids in phosphorus-limited conditions (Dembitsky, 1996). Higher concentrations were recorded in winter or spring months, which could indicate their enrichment in young algae observed from February only. This finding was consistent with a recent study, which showed that the total content

of DGTAs in the Ochrophyta *Sargassum horneri* increased during the growth phase and decreased when the alga became mature (Zhang *et al*., 2018). On the contrary, positive correlations were reported between the OTUs from the second cluster and some lipid classes, which were more produced in summer. These compounds were non-polar DAGs and TAGs, considered as energy and storage compounds, and ceramides. The occurrence of such lipids in the summer was not surprising as the accumulation of TAGs and their precursor DAGs in algae is known to occur under stress conditions, such as high light intensity, high salinity or N-deprivation (Liu and Benning, 2013). Among the wide range of biological roles, ceramides have also been characterized for their central role in response to biotic and abiotic stresses (Michaelson *et al*., 2016).

Unfortunately, several other metabolites which exhibited significant correlations with OTUs from the two clusters remained unidentified. This fact illustrated both the huge lack of molecular databases related to the marine organisms and the need to improve our knowledge on marine holobionts in order to better understand functions and roles associated with such complex living systems.

In conclusion, the meta-omics analysis performed here suggested that *T. atomaria* surface-associated microbiota was clearly specific and associated with key metabolites like DMSP, betaine or proline-betaine probably excreted by the host. In addition, despite a core community that represents a significant part of the total epibacteria, changes occurred in the structure of the community. In association with the increase in seawater temperature, these changes were connected to surface metabolome variations, suggesting that both environment and algae shape the bacterial surface microbiota. In the near future, if environmental drivers should be determined, the major challenge will be to improve the identification of key metabolites that will allow us to further understand how the actors of *T. atomaria* holobiont interact.

Experimental procedures

Algal material

The collection of *Taonia atomaria* algal specimens was carried out by hand (1 m depth) monthly during its occurrence period in the studied collection site (Carqueiranne, French Mediterranean coast, 43°5′12.41″N, 6°5′3.26″E) from February to July 2013. No thallus could be found in January or from August to December 2013. Following collection, three individual thalli were packed in 1 l-plastic bags filled with ambient seawater and transported in an isotherm container to the laboratory. From the point of collection, algal samples were treated within 2 h. Each month, three individual thalli of *T. atomaria* were collected as replicates. Each individual thallus was composed with several fronds and thus for each replicate one frond from a thallus was used for the metabolome extraction and another one from the same thallus was used for the DNA extraction.

Surface metabolome extraction, metabolomics analysis and data processing

The surface metabolome of samples of *T. atomaria* was obtained by a dipping method using methanol as an extraction solvent (Othmani *et al*., 2016a,b) (see Supporting Information for more details). A surface of approximately 10–12 cm^2 of one frond for each individual thallus was extracted for each month. It may be noted that, in the case of *T. atomaria*, the alternative solid phase extraction-based method previously described by Cirri *et al*. did not allow the detection of any compound by LC–MS (Cirri *et al*., 2016). The resulting surface extracts were concentrated under reduced pressure and stored at −20°C until analysis. Before injection, samples were solubilized in LC–MS grade methanol at a concentration of 10 mg ml^{-1}. Analytical blanks were also prepared and all samples were randomly injected to avoid systematic errors following the same injection sequence as that used in the study by Favre *et al*. (2017).

The metabolomic profiling was performed using a previously described experimental protocol (Favre *et al*., 2017), the sole difference being the elution gradient used. In the present study, the mobile phase gradient involved a binary programming of acidified acetonitrile (B) and water (A), containing each 0.1% of formic acid (v/v). The elution gradient started at 5% B, which was held for 2 min, and then increased to 100% B (linear ramp) within 8 min and maintained for 4 min; it was then reduced to 5% B over 0.01 min and maintained for 1.99 min, for a total run time of 16 min.

Raw UPLC/MS data were analysed using DataAnalysis (version 4.3; Bruker Daltonics), converted into netCDF files and processed for peak finding, integration and alignment using the open source XCMS package (version 1.46.0; Smith *et al*., 2006) in the R 3.2.3 environment. The resulting variables list was further processed by the CAMERA package (version 1.26.0) (Kuhl *et al*., 2012) and three successive filtering steps (signal/noise ratio, coefficient of variation and coefficient of autocorrelation between variables in a same given 'pcgroup') using an in-house script were run on R.

These variables were normalized by the sum, $\log_{10}$-transformed, mean-centred and analysed by principal component analysis (PCA) and partial least-square discriminant analysis (PLS-DA) using the MetaboAnalyst 3.5 online resource (http://www.metaboanalyst.ca). Analysed

data from MetaboAnalyst were then exported and figures were generated in the R 3.2.3 environment using the 'ggplot2' package. The seasonal clustering observed with PCA and PLS-DA scores plots were statistically tested respectively with PERMANOVA test (999 permutations) using the 'Vegan' R package, and a permutation test using MetaboAnalyst webtool (Separation distance: B/W, 1000 permutations). The variation of each selected metabolite during each month was then statistically tested by one-way ANOVA followed by post-hoc test (HSD) using the 'Agricolae' R package.

MS/MS molecular networking and annotation of metabolites

The MS/MS molecular network was generated on the GNPS online tool (https://gnps.ucsd.edu). Briefly, MS/MS data were clustered using default parameters for 'medium data preset' with a precursor ion mass tolerance of 2 Da and a fragment ion mass tolerance of 0.5 Da. Data were analysed using Cytoscape (version 3.4.0), with nodes to represent *m/z* detected features and edges to represent the MS/MS spectral similarity between *m/z* features. Normalized concentrations for metabolites found commonly within the molecular network were imported into Cytoscape. By implementing these data, a pie chart was generated into each node revealing the relative seasonal distribution of each metabolite. Transparency of edges connecting each node was proportional to the spectral similarity using a cosine score (CS).

In most metabolomics studies, and more particularly in the case of non-model organisms, the identification of VIPs and metabolome annotations are considered the limiting steps in the analytical workflow. In this study, annotation of the top discriminatory *m/z* features was undertaken using (i) a thorough analysis of HRMS data and MS fragmentation patterns, (ii) the construction of a molecular network based on MS/MS experiments and/or (iii) comparison of the MS and MS/MS data with free online databases (e.g. Metlin), including annotation tools such as MetFusion (Gerlich and Neumann, 2013), and with compounds that are commercially available or have already been isolated from *T. atomaria* or other algae by our research team (Viano *et al*., 2009; Othmani *et al*., 2016a,b). Using this methodology, 11 compounds were unambiguously annotated using chemical standards [four commercial standards: DMSP, proline betaine, proline and mannitol; seven natural compounds previously isolated in our laboratory (Othmani *et al*., 2016a,b) and 33 *m/z* features were putatively identified through molecular networking, the analysis of HRMS/MS data and comparison with databases and chemical standards (Supporting Information Dataset S1). All commercial standards were purchased from Sigma-Aldrich or Cayman Chemicals.

Epibacterial communities DNA extraction, amplification and sequencing

Each thallus was washed with phosphate buffered saline(PBS pH 7.4). A sterile scalpel was used to scrape off the epiphytic bacteria, which were introduced into plastic Eppendorf tubes (2 ml). A surface of approximately 10–12 cm^2 of one frond from each three individual thalli was scrapped for each month. Extraction of the bacterial DNA was carried out using the PowerBiofilm DNA isolation Kits (Qiagen). For each DNA extract, the V5-V6 region of the 16S rDNA was targeted using 5′ CAAACAGGATTAGATACCCTG 3′ (775F) and 3′ CGTTRCGGGACTTAACCCAACA 5′ (1103R) following (Youssef *et al*., 2009). The amplicons were paired-end sequenced (2 × 250 bp) on an Illumina MiSeq plaform (RTL, Texas). Sequences assessed in this study have been submitted to NCBI under the accession number SUB4952404.

Metabarcoding data processing and statistical analysis

The MiSeq data were assembled with the vsearch tool (https://github.com/torognes/vsearch) and the sequences were cleaned as follows: sequences were removed if they presented ambiguous bases 'N', a length shorter than 200 bp and had a mismatch in the forward and reverse primers. The putative chimaeras were detected by vsearch. The remaining rRNA 16S sequences were clustered into 'molecular species' (OTUs) at a 97% similarity threshold with vsearch (option cluster_small sorted by length) (Rognes *et al*., 2016). The representative sequence for each OTU was inserted into phylogenetic trees for taxonomic annotation. The seed OTUs were affiliated by similarity and phylogeny from reference sequences. These microbial references were extracted from the SSU SILVA database (Pruesse *et al*., 2007) according to the following criteria: length N 1200 bp, quality score N 75% and a pintail value N 50. After comparing the OTUs with the reference sequences using a similarity approach (vsearch tool), trees including OTUs with their closest references were built with FastTree (Price *et al*., 2010). The different taxonomic affiliations obtained were checked for inconsistency. This process was implemented using the pipeline Phylogenetic Analysis of Next-generation AMplicons (PANAM https://github.com/panammeb/PANAM2) and is described in more detail in the study by Taib *et al*. (2013).

Alpha-diversity metrics (Chao1, Shannon and Simpson indexes) were calculated using the Phyloseq R package and MicrobiomeAnalyst online tool (http://www.microbiomeanalyst.ca/) and tested statistically with a one-way ANOVA followed by a post hoc test (HSD) using the Agricolae R package. Dissimilarity matrices using the

Bray–Curtis distances were represented in a two-dimensional space by a principal coordinates analysis (PCoA). The similarity difference observed between each month with the PCoA was then statistically tested with a PERMANOVA test (999 permutations), using the Vegan R package.

Integration of metabolomic and metabarcoding data set

Correlation analysis between metabolomics and the metabarcoding data set was performed using the multi-block analysis DIABLO (block.splsda function) from MixOmics R package (Lê Cao *et al*., 2009). Briefly, the aim of this multivariate analysis was to perform an N-block integration of different -omics data sets to identify the most correlated variables involved in the discrimination of each group of samples. Here, this multi-block analysis allowed the most correlated OTUs and metabolites involved in the discrimination of each month to be identified. To perform such an analysis, an optimal number of variables (49 metabolites and 59 OTUs), which were the most involved in the seasonal discrimination, was specifically selected using the tuning function (tune.block.splsda function). The level of correlation between the two selected data sets was checked using the correlation coefficient calculated by the DIABLO analysis and a Mantel test ('ade4' R package).

Based on this analysis, a correlation network showing only positive (>0.7) and negative (<−0.7) correlations between the selected variables was built, and then imported and analysed with Cytoscape.

Acknowledgements

This work was supported by the Ministry of Higher Education and Scientific Research of Tunisia (A.O. PhD grant) and the French 'Provence-Alpes-Côte d'Azur (PACA) regional council (B.P. PhD grant). The authors are grateful to Dr S. Greff for his help during the acquisition of LC–MS profiles. LC–MS experiments were conducted on the regional platform MALLABAR funded by the Institute of Ecology and Environment (INEE) of the National Center for Scientific Research (CNRS) and the French PACA regional council.

References

Aires, T., Serrão, E.A., and Engelen, A.H. (2016) Host and environmental specificity in bacterial communities associated to two highly invasive marine species (genus *Asparagopsis*). *Front Microbiol* **7**: 559.

Astudillo-García, C., Bell, J.J., Webster, N.S., Glasl, B., Jompa, J., Montoya, J.M., and Taylor, M.W. (2017) Evaluating the core microbiota in complex communities: a systematic investigation. *Environ Microbiol* **19**: 1450–1462.

Baek, K., Choi, A., Kang, I., Im, M., and Cho, J.C. (2014) *Granulosicoccus marinus* sp nova, isolated from Antarctic seawater, and emended description of the genus *Granulosicoccus*. *Int J Syst Evol Microbiol* **64**: 4103–4108.

Barott, K.L., Rodriguez-Brito, B., Janouskovec, J., Marhaver, K.L., Smith, J.E., Keeling, P., and Rohwer, F.L. (2011) Microbial diversity associated with four functional groups of benthic reef algae and the reef-building coral *Montastraea annularis*. *Environ Microbiol* **13**: 1192–1204.

Bordenstein, S.R., and Theis, K.R. (2015) Host biology in light of the microbiome: ten principles of holobionts and hologenomes. *PLoS Biol* **13**: e1002226.

Briand, J.-F., Barani, A., Garnier, C., Réhel, K., Urvois, F., LePoupon, C., *et al*. (2017) Spatio-temporal variations of marine biofilm communities colonizing artificial substrata including antifouling coatings in contrasted French coastal environments. *Microb Ecol* **74**: 585–598.

Burke, C., Steinberg, P., Rusch, D., Kjelleberg, S., and Thomas, T. (2011a) Bacterial community assembly based on functional genes rather than species. *Proc Natl Acad Sci* **108**: 14288–14293.

Burke, C., Thomas, T., Lewis, M., Steinberg, P., and Kjelleberg, S. (2011b) Composition, uniqueness and variability of the epiphytic bacterial community of the green alga *Ulva australis*. *ISME J* **5**: 590–600.

Chang, Y.-C., and Lee, T.-M. (1999) High temperature-induced free proline accumulation in *Gracilaria tenuistipitata* (Rhodophyta). *Bot Bull Acad Sini* **40**: 289–294.

Cirri, E., Grosser, K., and Pohnert, G. (2016) A solid phase extraction based non-disruptive sampling technique to investigate the surface chemistry of macroalgae. *Biofouling* **32**: 145–153.

Dang, H., and Lovell, C.R. (2016) Microbial surface colonization and biofilm development in marine environments. *Microbiol Mol Biol Rev* **80**: 91–138.

Dembitsky, V.M. (1996) Betaine ether-linked glycerolipids: chemistry and biology. *Prog Lipid Res* **35**: 1–51.

Dittami, S., Gravot, A., Renault, D., Goulitquer, S., Eggert, A., Bouchereau, A., *et al*. (2011) Integrative analysis of metabolite and transcript abundance during the short-term response to saline and oxidative stress in the brown alga *Ectocarpus siliculosus*. *Plant Cell Environ* **34**: 629–642.

Egan, S., Harder, T., Burke, C., Steinberg, P., Kjelleberg, S., and Thomas, T. (2013) The seaweed holobiont: understanding seaweed-bacteria interactions. *FEMS Microbiol Rev* **37**: 462–476.

Favre, L., Ortalo-Magné, A., Greff, S., Pérez, T., Thomas, O. P., Martin, J.-C., and Culioli, G. (2017) Discrimination of four marine biofilm-forming bacteria by LC–MS metabolomics and influence of culture parameters. *J Proteome Res* **16**: 1962–1975.

Fernandes, N., Case, R.J., Longford, S.R., Seyedsayamdost, M.R., Steinberg, P.D., Kjelleberg, S., and Thomas, T. (2011) Genomes and virulence factors of novel bacterial pathogens causing bleaching disease in the marine red alga *Delisea pulchra*. *PLoS One* **6**: e27387.

Fernandes, N., Steinberg, P., Rusch, D., Kjelleberg, S., and Thomas, T. (2012) Community structure and functional gene profile of bacteria on healthy and diseased thalli of the red seaweed *Delisea pulchra*. *PLoS One* **7**: e50854.

Florez, J.Z., Camus, C., Hengst, M.B., and Buschmann, A.H. (2017) A functional perspective analysis of macroalgae

and epiphytic bacterial community interaction. *Front Microbiol* **8**: 2561.

Flot, J.F., Bauermeister, J., Brad, T., Hillebrand-Voiculescu, A., Sarbu, S.M., and Dattagupta, S. (2014) *Niphargus-Thiothrix* associations may be widespread in sulphidic groundwater ecosystems: evidence from south-eastern Romania. *Mol Ecol* **23**: 1405–1417.

Gerlich, M., and Neumann, S. (2013) MetFusion: integration of compound identification strategies. *J Mass Spectrom* **48**: 291–298.

Ghaderiardakani, F., Coates, J.C., and Wichard, T. (2017) Bacteria-induced morphogenesis of *Ulva intestinalis* and *Ulva mutabilis* (Chlorophyta): a contribution to the lottery theory. *FEMS Microbiol Ecol* **93**: fix094.

Gillan, D.C., and Dubilier, N. (2004) Novel epibiotic *Thiothrix* bacterium on a marine amphipod. *Appl Environ Microbiol* **70**: 3772–3775.

Grueneberg, J., Engelen, A.H., Costa, R., and Wichard, T. (2016) Macroalgal morphogenesis induced by waterborne compounds and bacteria in coastal seawater. *PLoS One* **11**: e0146307.

Harder, T., Campbell, A.H., Egan, S., and Steinberg, P.D. (2012) Chemical mediation of ternary interactions between marine holobionts and their environment as exemplified by the red alga *Delisea pulchra*. *J Chem Ecol* **38**: 442–450.

Hollants, J., Leliaert, F., De Clerck, O., and Willems, A. (2013) What we can learn from sushi: a review on seaweed–bacterial associations. *FEMS Microbiol Ecol* **83**: 1–16.

Huang, R., Zhou, X., Xu, T., Yang, X., and Liu, Y. (2010) Diketopiperazines from marine organisms. *Chem Biodivers* **7**: 2809–2829.

Johnson, C.H., Ivanisevic, J., and Siuzdak, G. (2016) Metabolomics: beyond biomarkers and towards mechanisms. *Nat Rev Mol Cell Biol* **17**: 451–459.

Karsten, U., Kirst, G.O., and Wiencke, C. (1992) Dimethylsulphoniopropionate (DMSP) accumulation in green macioalgae from polar to temperate regions: interactive effects of light versus salinity and light versus temperature. *Polar Biol* **12**: 603–607.

Kessler, R.W., Crecelius, A.C., Schubert, U.S., and Wichardet, T. (2017) In situ monitoring of molecular changes during cell differentiation processes in marine macroalgae through mass spectrometric imaging. *Anal Bioanal Chem* **409**: 4893–4903.

Kessler, R.W., Weiss, A., Kuegler, S., Hermes, C., and Wichard, T. (2018) Macroalgal–bacterial interactions: role of dimethylsulfoniopropionate in microbial gardening by Ulva (Chlorophyta). *Mol Ecol* **27**: 1808–1819.

Konkol, N.R., Bruckner, J.C., Aguilar, C., Lovalvo, D., and Maki, J.S. (2010) Dominance of epiphytic filamentous *Thiothrix* spp. on an aquatic macrophyte in a hydrothermal vent flume in Sedge Bay, Yellowstone Lake, Wyoming. *Microb Ecol* **60**: 528–538.

Kuhl, C., Tautenhahn, R., Böttcher, C., Larson, T.R., and Neumann, S. (2012) CAMERA: an integrated strategy for compound spectra extraction and annotation of liquid chromatography/mass spectrometry data sets. *Anal Chem* **84**: 283–289.

Lachnit, T., Fischer, M., Künzel, S., Baines, J.F., and Harder, T. (2013) Compounds associated with algal surfaces mediate epiphytic colonization of the marine macroalga *Fucus vesiculosus*. *FEMS Microbiol Ecol* **84**: 411–420.

Lachnit, T., Meske, D., Wahl, M., Harder, T., and Schmitz, R. (2011) Epibacterial community patterns on marine macroalgae are host-specific but temporally variable. *Environ Microbiol* **13**: 655–665.

Lê Cao, K.-A., González, I., and Déjean, S. (2009) integrOmics: an R package to unravel relationships between two omics datasets. *Bioinformatics* **25**: 2855–2856.

Lemay, M.A., Martone, P.T., Keeling, P.J., Burt, J.M., Krumhansl, K.A., Sanders, R.D., and Parfrey, L.W. (2018) Sympatric kelp species share a large portion of their surface bacterial communities. *Environ Microbiol* **20**: 658–670.

Li, H.R., Yu, Y., Luo, W., Zeng, Y.X., and Chen, B. (2009) Bacterial diversity in surface sediments from the Pacific Arctic Ocean. *Extremophiles* **13**: 233–246.

Liu, B.S., and Benning, C. (2013) Lipid metabolism in microalgae distinguishes itself. *Curr Opin Biotechnol* **24**: 300–309.

Lyons, D.A., Scheibling, R.E., and Van Alstyne, K.L. (2010) Spatial and temporal variation in DMSP content in the invasive seaweed *Codium fragile ssp fragile*: effects of temperature, light and grazing. *Mar Ecol Prog Ser* **417**: 51–61.

Marzinelli, E.M., Campbell, A.H., Zozaya Valdes, E., Vergés, A., Nielsen, S., Wernberg, T., *et al*. (2015) Continental-scale variation in seaweed host-associated bacterial communities is a function of host condition, not geography. *Environ Microbiol* **17**: 4078–4088.

Matsuo, Y., Imagawa, H., Nishizawa, M., and Shizuri, Y. (2005) Isolation of an algal morphogenesis inducer from a marine bacterium. *Science* **307**: 1598–1598.

McNeil, S.D., Nuccio, M.L., and Hanson, A.D. (1999) Betaines and related osmoprotectants. Targets for metabolic engineering of stress resistance. *Plant Physiol* **120**: 945–949.

Michaelson, L.V., Napier, J.A., Molino, D., and Faure, J.D. (2016) Plant sphingolipids: their importance in cellular organization and adaption. *BBA-Mol Cell Biol L* **1861**: 1329–1335.

Michelou, V.K., Caporaso, J.G., Knight, R., and Palumbi, S.R. (2013) The ecology of microbial communities associated with *Macrocystis pyrifera*. *PLoS One* **8**: e67480.

Nelson, C.E., Carlson, C.A., Ewart, C.S., and Halewood, E. R. (2014) Community differentiation and population enrichment of Sargasso Sea bacterioplankton in the euphotic zone of a mesoscale mode-water eddy. *Environ Microbiol* **16**: 871–887.

Oberbeckmann, S., Kreikemeyer, B., and Labrenz, M. (2018) Environmental factors support the formation of specific bacterial assemblages on microplastics. *Front Microbiol* **8**: 2709.

Ortiz-Castro, R., Diaz-Perez, C., Martinez-Trujillo, M., del Rio, R.E., Campos-Garcia, J., and Lopez-Bucio, J. (2011) Transkingdom signaling based on bacterial cyclodipeptides with auxin activity in plants. *Proc Natl Acad Sci U S A* **108**: 7253–7258.

Othmani, A., Briand, J.F., Aye, M., Molmeret, M., and Culioli, G. (2016a) Surface metabolites of the brown alga *Taonia atomaria* have the ability to regulate epibiosis. *Biofouling* **32**: 801–813.

Othmani, A., Bunet, R., Bonnefont, J.L., Briand, J.F., and Culioli, G. (2016b) Settlement inhibition of marine biofilm bacteria and barnacle larvae by compounds isolated from the Mediterranean brown alga *Taonia atomaria*. *J Appl Phycol* **28**: 1975–1986.

Park, S., Jung, Y.T., Won, S.M., Park, J.M., and Yoon, J.H. (2014) *Granulosicoccus undariae* sp nov., a member of the family Granulosicoccaceae isolated from a brown algae reservoir and emended description of the genus *Granulosicoccus*. *Anton Leeuw Int J Gen Mol Microbiol* **106**: 845–852.

Pollet, T., Berdjeb, L., Garnier, C., Durrieu, G., Le Poupon, C., Misson, B., and Briand, J.-F. (2018) Prokaryotic community successions and interactions in marine biofilms: the key role of Flavobacteriia. *FEMS Microbioly Ecol* **94**: fiy083.

Price, M.N., Dehal, P.S., and Arkin, A.P. (2010) FastTree 2 – approximately maximum-likelihood trees for large alignments. *PLoS One* **5**: e9490.

Pruesse, E., Quast, C., Knittel, K., Fuchs, B.M., Ludwig, W. G., Peplies, J., and Glockner, F.O. (2007) SILVA: a comprehensive online resource for quality checked and aligned ribosomal RNA sequence data compatible with ARB. *Nucleic Acids Res* **35**: 7188–7196.

Rickert, E., Karsten, U., Pohnert, G., and Wahl, M. (2015) Seasonal fluctuations in chemical defenses against macrofouling in *Fucus vesiculosus* and *Fucus serratus* from the Baltic Sea. *Biofouling* **31**: 363–377.

Rickert, E., Lenz, M., Barboza, F.R., Gorb, S.N., and Wahl, M. (2016b) Seasonally fluctuating chemical microfouling control in *Fucus vesiculosus* and *Fucus serratus* from the Baltic Sea. *Mar Biol* **163**: 13.

Rickert, E., Wahl, M., Link, H., Richter, H., and Pohnert, G. (2016a) Seasonal variations in surface metabolite composition of *Fucus vesiculosus* and *Fucus serratus* from the Baltic Sea. *PLoS One* **11**: 18.

Rizzo, L., Fraschetti, S., Alifano, P., Pizzolante, G., and Stabili, L. (2016) The alien species *Caulerpa cylindracea* and its associated bacteria in the Mediterranean Sea. *Mar Biol* **163**: 4.

Roche, S.A., and Leblond, J.D. (2010) Betaine lipids in chlorarachniophytes. *Phycological Research* **58**: 298–305. https://doi.org/10.1111/j.1440-1835.2010.00590.x

Rognes, T., Flouri, T., Nichols, B., Quince, C., and Mahé, F. (2016) VSEARCH: a versatile open source tool for metagenomics. *PeerJ* **4**: e2584.

Rosenberg, E., Koren, O., Reshef, L., Efrony, R., and Zilber-Rosenberg, I. (2007) The role of microorganisms in coral health, disease and evolution. *Nat Rev Microbiol* **5**: 355–362.

Saha, M., Rempt, M., Gebser, B., Grueneberg, J., Pohnert, G., and Weinberger, F. (2012) Dimethylsulphopropionate (DMSP) and proline from the surface of the brown alga *Fucus vesiculosus* inhibit bacterial attachment. *Biofouling* **28**: 593–604.

Saha, M., Rempt, M., Grosser, K., Pohnert, G., and Weinberger, F. (2011) Surface-associated fucoxanthin mediates settlement of bacterial epiphytes on the rockweed *Fucus vesiculosus*. *Biofouling* **27**: 423–433.

Saha, M., Rempt, M., Stratil, S.B., Wahl, M., Pohnert, G., and Weinberger, F. (2014) Defence chemistry modulation by light and temperature shifts and the resulting effects on associated epibacteria of *Fucus vesiculosus*. *PLoS One* **9**: e105333.

Sala, E., and Boudouresque, C.F. (1997) The role of fishes in the organization of a Mediterranean sublittoral community.1. Algal communities. *J Exp Mar Biol Ecol* **212**: 25–44.

Smith, C.A., Want, E.J., O'Maille, G., Abagyan, R., and Siuzdak, G. (2006) XCMS: processing mass spectrometry data for metabolite profiling using nonlinear peak alignment, matching, and identification. *Anal Chem* **78**: 779–787.

Sneed, J.M., Ritson-Williams, R., and Paul, V.J. (2015) Crustose coralline algal species host distinct bacterial assemblages on their surfaces. *ISME J* **9**: 2527–2536.

Spoerner, M., Wichard, T., Bachhuber, T., Stratmann, J., and Oertel, W. (2012) Growth and thallus morphogenesis of *Ulva mutabilis* (Chlorophyta) depends on a combination of two bacterial species excreting regulatory factors. *J Phycol* **48**: 1433–1447.

Spring, S., Scheuner, C., Göker, M., and Klenk, H.-P. (2015) A taxonomic framework for emerging groups of ecologically important marine gammaproteobacteria based on the reconstruction of evolutionary relationships using genome-scale data. *Front Microbiol* **6**: 281.

Stratil, S.B., Neulinger, S.C., Knecht, H., Friedrichs, A.K., and Wahl, M. (2013) Temperature-driven shifts in the epibiotic bacterial community composition of the brown macroalga *Fucus vesiculosus*. *Microbiol Open* **2**: 338–349.

Stratil, S.B., Neulinger, S.C., Knecht, H., Friedrichs, A.K., and Wahl, M. (2014) Salinity affects compositional traits of epibacterial communities on the brown macroalga *Fucus vesiculosus*. *FEMS Microbiol Ecol* **88**: 272–279.

Taib, N., Mangot, J.-F., Domaizon, I., Bronner, G., and Debroas, D. (2013) Phylogenetic affiliation of SSU rRNA genes generated by massively parallel sequencing: new insights into the freshwater protist diversity. *PLoS One* **8**: e58950.

Theis, K.R., Dheilly, N.M., Klassen, J.L., Brucker, R.M., Baines, J.F., Bosch, T.C.G., *et al*. (2016) Getting the hologenome concept right: an eco-evolutionary framework for hosts and their microbiomes. *mSystems* **1**: e00028–e00016.

Verhoeven, J.T.P., Kavanagh, A.N., and Dufour, S.C. (2017) Microbiome analysis shows enrichment for specific bacteria in separate anatomical regions of the deep-sea carnivorous sponge *Chondrocladia grandis*. *FEMS Microbiol Ecol* **93**: fiw214.

Viano, Y., Bonhomme, D., Camps, M., Briand, J.-F., Ortalo-Magné, A., Blache, Y., *et al*. (2009) Diterpenoids from the Mediterranean brown alga *Dictyota* sp. evaluated as antifouling substances against a marine bacterial biofilm. *J Nat Prod* **72**: 1299–1304.

Vieira, C., Engelen, A.H., Guentas, L., Aires, T., Houlbreque, F., Gaubert, J., *et al*. (2016) Species specificity of bacteria associated to the brown seaweeds *Lobophora* (Dictyotales, Phaeophyceae) and their

potential for induction of rapid coral bleaching in *Acropora muricata*. *Front Microbiol* **7**: 316.

Wahl, M., Goecke, F., Labes, A., Dobretsov, S., and Weinberger, F. (2012) The second skin: ecological role of epibiotic biofilms on marine organisms. *Front Microbiol* **3**: 292.

Wang, L., Liu, X.S., Yu, S.L., Shi, X.C., Wang, X.L., and Zhang, X.H. (2017) Bacterial community structure in intertidal sediments of Fildes peninsula, maritime Antarctica. *Polar Biol* **40**: 339–349.

Wang, M., Carver, J.J., Phelan, V.V., Sanchez, L.M., Garg, N., Peng, Y., *et al*. (2016) Sharing and community curation of mass spectrometry data with global natural products social molecular networking. *Nat Biotechnol* **34**: 828–837.

Wichard, T., and Beemelmanns, C. (2018) Role of chemical mediators in aquatic interactions across the prokaryote–eukaryote boundary. *J Chem Ecol* **44**: 1008–1021.

Youssef, N., Sheik, C.S., Krumholz, L.R., Najar, F.Z., Roe, B.A., and Elshahed, M.S. (2009) Comparison of species richness estimates obtained using nearly complete fragments and simulated pyrosequencing-generated fragments in 16S rRNA gene-based environmental surveys. *Appl Environ Microbiol* **75**: 5227–5236.

Zhang, P., Wang, X., Wang, T., Zhu, P., and Yang, L. (2018) The major changes in lipid composition of *Sargassum horneri* during different growth phases. *J Appl Phycol* **30**: 517–523.

Zozaya-Valdes, E., Roth-Schulze, A.J., Egan, S., and Thomas, T. (2017) Microbial community function in the bleaching disease of the marine macroalgae *Delisea pulchra*. *Environ Microbiol* **19**: 3012–3024.

Supporting Information

Additional Supporting Information may be found in the online version of this article at the publisher's web-site:

Supplementary Dataset S1

Fig. S1. Chemical structures of some surface metabolites isolated from *T. atomaria*

Fig. S2. (+)-ESI-LC–MS profiles of surface extracts of *T. atomaria* (collected monthly from February to July)

Fig. S3. PCA score plot obtained from (+)-ESI-LC–MS profiles of surface extracts of *T. atomaria* collected monthly from February to July (n = 18), QCs sample (n = 8) and blanks (solvent blanks, n = 2; analytical blanks, n = 4)

Fig. S4. PLS-DA analysis from (+)-ESI-LC–MS profiles of surface extracts of *T. atomaria* collected monthly from February to July (one class per month). Since the analysis involved a time series, the 'Class order matters' option was checked. (A) show the PLS-DA scores plot. (B) show the VIPs scores of the 100 first VIPs according to their ranks. The rectangle (in red) show the 18 first VIPs above the regression line (in green) and selected for the analysis. (C) show the permutation test results (Separation distance: B/W, 1000 permutations).

Fig. S5. HRMS/MS data and hypothetical MS fragmentation of VIP n°1 putatively identified as Proline betaine

Fig. S6. HRMS/MS data and hypothetical MS fragmentation of VIP n°2 identified as DMSP

Fig. S7. HRMS/MS data and hypothetical MS fragmentation of VIP n°3 putatively identified as Ceramide (dC18:1/C16:0)

Fig. S8. HRMS/MS data and hypothetical MS fragmentation of VIP n°4 putatively identified as DGTA (C44:10)

Fig. S9. HRMS/MS data and MS fragmentation of VIP n°5 identified as Proline

Fig. S10. HRMS/MS data and hypothetical MS fragmentation of VIP n°6 putatively identified as DGTA (C44:12)

Fig. S11. HRMS/MS data of VIP n°7 identified as Sesquiterpene IV

Fig. S12. HRMS/MS data of VIP n°8

Fig. S13. HRMS/MS data and hypothetical MS fragmentation of VIP n°9 putatively identified as *Lyso*-DGTA (C20:5)

Fig. S14. HRMS/MS data and hypothetical MS fragmentation of VIP n°10 putatively identified as Glutaminevaline (Gln-Val)

Fig. S15. HRMS/MS data of VIP n°11

Fig. S16. HRMS/MS data and hypothetical MS fragmentation of VIP n°12 putatively identified as Ceramide (dC18:1/C14:0)

Fig. S17. HRMS/MS data and hypothetical MS fragmentation of VIP n°13 putatively identified as Glutamineleucine (Gln-Leu)

Fig. S18. HRMS/MS data and hypothetical MS fragmentation of VIP n°14 putatively identified as DGTA (C32:2)

Fig. S19. HRMS/MS data and hypothetical MS fragmentation of VIP n°15

Fig. S20. HRMS/MS data and hypothetical MS fragmentation of VIP n°16 identified as Glutaminephenylalanine (Gln-Phe)

Fig. S21. HRMS/MS data of VIP n°17

Fig. S22. HRMS/MS data and hypothetical MS fragmentation of VIP n°18 identified as difucol-2-*O*-sulfate

Fig. S23. Seasonal variations (from February to July) of the epibacterial communities on *T. atomaria* at the class level. A, B, C represent biological replicates.

Fig. S24. Seasonal variations of the relative abundance of the core microbiome of *T. atomaria.* A: percentage of sequences, B: percentage of OTUs). Standard deviation represented the variation in the three replicates.

Fig. S25. Heatmap representation of the seasonal correlation (multi-block PLS-DA) between significant OTUs and metabolites found at the surface of *T. atomaria*